Research and Development of Emerging Technologies for Exosome-based Cancer Diagnostics and Therapeutics

Sergio Ayala-Mar, MD, PhD[1] and José González-Valdez, PhD[2]
[1,2]Tecnológico de Monterrey, Mexico, sergio.ayala@tec.mx, jose_gonzalez@tec.mx

***Abstract*– Exosomes, which are extracellular vesicles involved in transferring biomolecules between cells and tissues, hold great potential as diagnostic and therapeutic tools in cancer. However, there are challenges in bringing exosome technology to clinical practice. This work tackles these challenges through a multidisciplinary approach, focusing on enhancing exosome isolation, controlled delivery, and studying exosome biogenesis. Therefore, this work involves the development of microfluidic technology, a biomaterial-based delivery system, and a 3D cell culture model to study exosome biology.**

Keywords—Exosomes; Nanomedicine; Cancer; Microfluidics; Biomaterials

I. Introduction

Extracellular vesicles (EVs) can be regarded as natural nanomaterials that can be used in various biomedical applications, including nanomedicine. EVs are cellular nanoparticles that are released by all cell types into the extracellular space.

Because of their properties and function, EVs have been proposed as specific carriers for therapeutic agents and biomarkers for health and disease [1]. Particularly, exosomes have gained particular attention because of their unique biogenesis, conserved composition, and high stability.

Exosomes are typically 30-150 nanometers in diameter and are thought to contain a variety of specific biomolecules, which can provide insight into the state of cellular homeostasis. Recent studies have demonstrated the potential of exosomes as diagnostic and therapeutic tools [2], [3]. These EVs can be isolated from a wide variety of biological fluids, and their contents can be analyzed to identify biomarkers for disease diagnosis and prognosis. Modified exosomes can also be engineered for therapeutic applications.

Nanomedicine and exosome research overlap, as both fields explore the by using of nanomaterials to address prevalent public health problems, such as cancer. Cancer nanomedicine involves the use of nanotechnology to develop diagnostics and therapeutics to overcome the current limitations of cancer care [4].

Cancer treatment is a multifaceted process, which reflects the complexity of this disease [4]. Cancer can arise in any tissue and can spread throughout the body. It is often not detected until it has already progressed to an advanced stage, and it is fundamentally different in every patient. Thus, early detection and personalized treatments are needed to improve clinical outcomes.

Despite the impressive progress made in exosome research, there is a gap between the bast body of literature outlining the potential applications of exosomes and its clinical translation. This can be attributed to several challenges faced by this field, including lack of standardization in exosome isolation, characterization and functional analysis, a limited understanding of their biology, toxicity, targeting specificity, and costs associated to manufacturing [5]–[7].

Solving these issues requires a multidisciplinary approach, as well as significant investment in research and development. Certainly, the development of new technologies to manipulate complex biological systems at the nanoscale is required to advance exosome research.

In this context, microfluidics has shown great potential for the isolation, characterization, and analysis of exosomes. Microfluidic devices allow the rapid and efficient isolation of exosomes, as well as analysis for diagnostics [8]. Furthermore, these devices can be designed for point-of-care testing.

Exosomes have also shown great potential as therapeutics. However, the lack of control over their biodistribution and pharmacokinetics can limit their therapeutic use and lead to off-target effects [9]. Controlled-delivery systems can address these limitations by allowing the control of exosome release at the target site.

Hydrogels are biomaterials composed by a three-dimensional network of hydrophilic polymer chains that are capable of absorbing and retaining water, which makes them suitable for a wide range of applications, including drug diffusion [10].

A potential approach is to use exosome-loaded hydrogels to deliver therapeutics directly to the target site. These exosome-hydrogel systems can be produced to degrade over time, releasing the exosomes into the surrounding tissue during a specific period.

Although a significant investment of resources has been dedicated to produce exosome-based diagnostics and therapeutics, the mechanisms of exosome biogenesis and function are not completely understood. The study of exosome biology can provide insights for cancer research, leading to the development of new therapeutic strategies, and improving the clinical translation of exosome-based nanomedicine.

Over the last decade, the development of various tissue-engineering techniques has allowed to produce next-generation drug screening platforms that also promise to increase our understanding of cancer biology [11]. Three-dimensional (3D) cell culture models, such as spheroids, organoids, and tissue-on-a-chip platforms allow researchers to mimic the complex biological conditions of tumors *in vitro*. 3D cell culture models can also provide better insights into exosome biogenesis and function in cancer.

Recent studies show that tumor-derived exosomes can promote cancer progression and have been associated to

therapeutic resistance [12]. In this context, exosomes have emerged as a potential target for cancer treatment.

Several strategies have been developed to inhibit exosome release by modulating the expression or function of molecules involved in their biogenesis [13]. This approach has also been proposed to study the mechanisms of exosome biogenesis, in particular cargo sorting, which has been associated to the subcellular localization of molecular targets for cancer therapeutics.

As noted by the development of 3D cell culture technology, technological advances are also required to fully understand the function of exosomes in cancer and to design novel therapeutic strategies. Fig. 1 shows an overview on how life science technology can be integrated to realize the full potential of exosomes to improve cancer care.

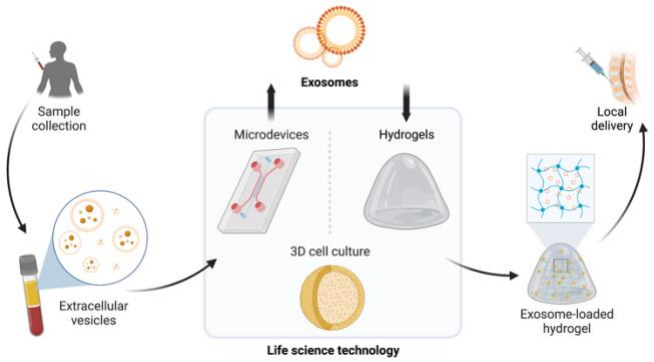

Fig. 1. Life science technology to advance exosome research.

Accordingly, we aimed to approach exosome research by addressing various challenges that limit the use of exosomes in various biomedical applications, through the development of technology. To achieve this goal, we provided proof of concept on the development of a microdevice for exosome isolation, a biomaterial-based delivery system for the controlled release of exosomes, and a 3D cell culture model to study exosome biology.

Firstly, we assumed that exosomes as nanoscale vesicles are well-suited for isolation in microfluidic devices, which can handle small sample volumes and achieve high control levels over fluid and particle movement. Therefore, the engineering of microfluidic technology for the isolation of exosomes based on their physicochemical properties will result in a rapid, precise, and simple method for exosome separation and concentration.

Next, we proposed that hydrogels can provide a suitable environment for exosome delivery because of their physicochemical properties, which facilitate the diffusion of exosomes and provides sustained release over time. Therefore, hydrogels can be engineered with tunable degradability, allowing the controlled release of exosomes over a defined period.

Finally, we assumed that 3D cell culture techniques will more accurately mimic *in vivo* conditions, thereby providing a more suitable model for studying exosome biology. By developing an 3D cell culture model to study the effect of exosome blockade, we can gain insights into the use of this novel strategy for combinatorial therapeutic approaches.

Based on the previously described assumptions, this work comprises three studies. Below, we provide a brief introduction and a summary of the methodology, experimental results, and conclusions for each study.

Digital Object Identifier: (only for full papers, inserted by LACCEI).
ISSN, ISBN: (to be inserted by LACCEI).
DO NOT REMOVE

II. Design and Optimization of an Electrical-Based Microfluidic Device for the Isolation of Exosomes

A. Introduction

Exosome isolation is the initial step in analyzing these EVs for their potential applications in cancer care. Electrical-based microdevices, particularly those utilizing dielectrophoresis (DEP), provide a simpler alternative to traditional methods, eliminating the need for specialized reagents and complex instrumentation [14].

DEP works by subjecting particles to non-uniform electric fields, resulting in their transport based on polarization effects [15]. Insulator-based DEP (iDEP) employs electrically insulating posts within the microchannel to create a non-uniform electric field, enabling effective manipulation of nanoparticles [16]. iDEP-based microdevices often utilize direct current (DC) fields to generate electroosmotic flow (EOF) for fluid movement.

Reference [17] includes the full description of this study. Here, we developed a microfluidic device based on insulator-based dielectrophoresis (iDEP) driven by direct current (DC) to isolate exosomes. Our aim was to achieve particle separation based on size by designing a microdevice with different sections of electrically insulating structures.

To facilitate sample recovery, our microdevice incorporated side channels with recovery reservoirs adjacent to each section of electrically insulating posts. Our findings show that microfluidics is a promising technology for concentrating and separating exosome subpopulations, thereby creating new opportunities for studying their roles in health and disease. Furthermore, this approach allows the isolation of exosomes with a narrow size distribution from larger plasma-membrane derived vesicles, potentially improving sample purity.

B. Experimental section

Microdevice design and fabrication. The microdevice was fabricated through a combination of photolithography and soft lithography techniques [17]. Polydimethylsiloxane (PDMS) was employed as the main material for device fabrication. The microdevice used in this study was designed with a main channel that included inlet and outlet reservoirs, as well as two sections of oval-shaped electrically insulating posts with different gap spaces (Fig. 2). The first post array had a 15 μm gap space, while the second array had a 10 μm gap space. The microchannel design was created using Autodesk AutoCAD software and printed as a mask.

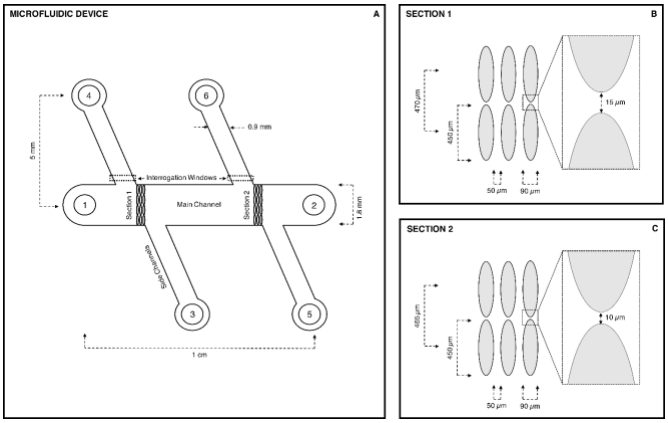

Figure 2. Schematic representation of the microdevice. Reprinted with permission from Ref [17]. Copyright 2023 American Chemical Society

Exosome isolation and characterization. MCF-7 cell line was cultured in Dulbecco's Modified Eagle Media (DMEM) supplemented with exosome-free fetal bovine serum (ED-FBS), (Gibco, USA). The cell culture medium was harvested, clarified, and concentrated according to reported protocols [17]. Exosomes were isolated using the Total Exosome Isolation reagent (TEI, Invitrogen, USA). The size distribution of the exosomes was evaluated through dynamic light scattering (DLS) using a Zeta Sizer Nano SP (Malvern Panalytical, UK).

Dielectrophoretic experiments, image analysis and statistical analysis. Exosome visualization during dielectrophoretic experiments was achieved using the fluorescent probe BODIPY TR ceramide (Invitrogen, USA) [17]. Exosomes were loaded into the microchannels, and DC voltages were applied across the main (1500-2000 V, for 20 s) and side channels (200 V, for 1 min) using platinum wire electrodes.

The images of the process were captured using a Nikon Eclipse Ti-2 inverted fluorescence microscope (Nikon Instruments Inc. USA). Statistical analysis was conducted using a one-way analysis of variance (ANOVA) and the student's t-test. A significance level of $P<0.05$ was considered statistically significant. Prism 8 (GraphPad, USA) software were used for the statistical analysis and graph generation. The measurements are presented as the mean of the replicates and their standard deviation (SD). Numerical simulations. The previously described geometry was reproduced in COMSOL Multiphysics 5.3a (COMSOL Inc., MA, USA) and analyzed using the electric currents study from the AC/DC module.

C. Results and discussion

Fig. 3A and 3B shows the streamlines and trapping of exosomes in the first and second sections, respectively, after a voltage of 1500 V was applied across the main channel. By increasing the voltage to 2000 V, the magnitude of the field gradient and the strength of the dielectrophoretic force were enhanced, enabling exosome trapping in both sections, as shown in Fig 3C and 3D.

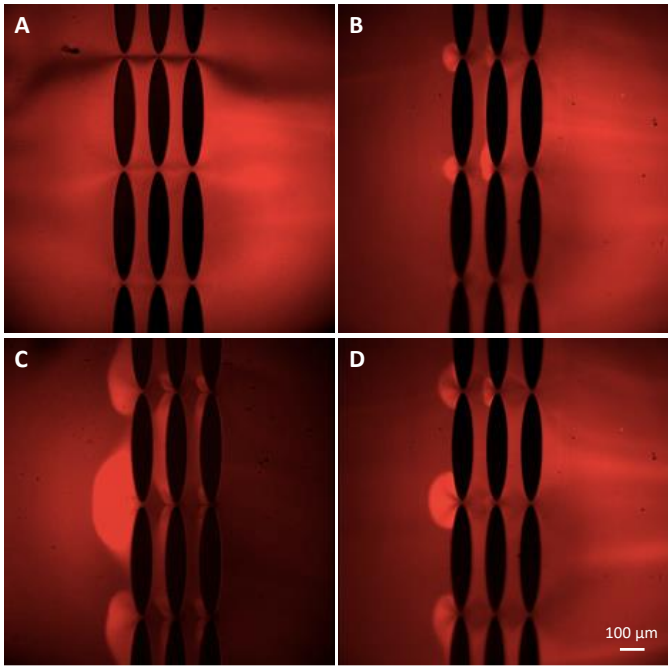

Figure 3. Fluorescence images depicting the dielectrophoretic response of exosomes in both sections after applying two different DC voltages. Reprinted with permission from Ref [17]. Copyright 2023 American Chemical Society

The concentration of exosomes in regions preceding the gap between posts indicated the interplay between the electric potential (EP) force and electroosmotic (EOF) flow played a role in exosome trapping, with EP contributing to trapping and EOF being the predominant component of the electrokinetic (EK) effect. Release of the sample and subsequent application of 200 V to the side channels directed the previously concentrated particles to their respective recovery reservoirs.

The separation efficiency of the device was assessed by comparing the mean diameters of exosomes from the inlet reservoir and the recovered fractions. The results confirmed size-based fractioning of exosomes, with the mean diameter in the first section being larger than in the inlet reservoir and significantly smaller in the second section, as shown in Fig 4A and 4B.

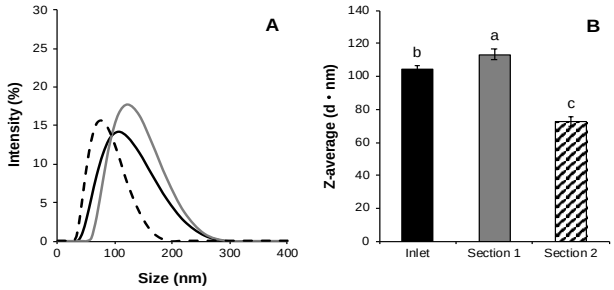

Figure 4. DLS measurements comparing particle size between the sample and the recovered fractions. The color of the lines in the size distributions corresponds to the bars in the pooled data comparisons. (A) Representative comparison between the particle size distribution from each fraction. (B) Pooled data of Z-average, showing mean particle diameter in each fraction. Reprinted with permission from Ref [17]. Copyright 2023 American Chemical Society

Next, we focused on the characterization of the electric field gradients required for trapping and separating exosomes using numerical simulations. The results showed that the highest magnitude of the field gradient, was achieved in the second section of the device because of the smaller gaps between the posts (Fig 5). Increasing the voltage to 2000 V led to simultaneous trapping in both sections. The field gradient magnitudes achieved were in the order of $3.3x10^{17}$ V^2/m^3 and $9.0x10^{17}$ V^2/m^3 in the first and second sections, respectively.

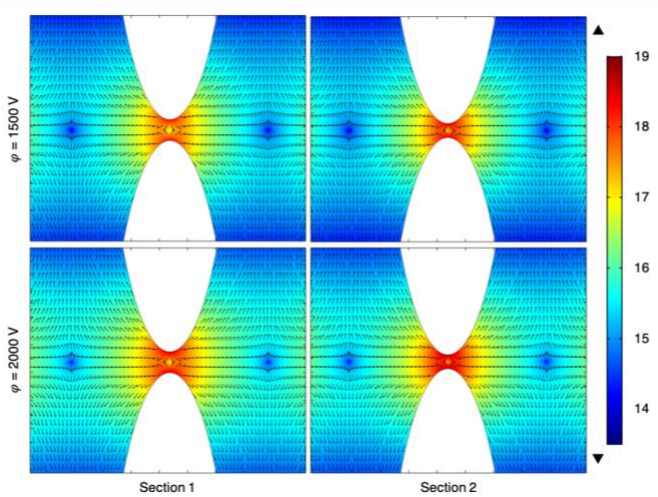

Fig 5. Numerical simulations. Field gradient spatial distribution in the vicinity of gaps between PDMS posts in the first and second section when applying voltages of 1500 V and 2000 V. Reprinted with permission from Ref [17]. Copyright 2023 American Chemical Society

D. Conclusion

This study presented a multi-section microfluidic device that successfully achieved simultaneous separation and concentration of exosomes using induced dielectrophoresis (iDEP). The device captured and separated exosomes based on their particle size, with larger exosomes being trapped in the first section and smaller exosomes in the second section.

The trapping and separation process was facilitated by the repulsive force generated in the gaps between electrically insulating posts, counteracting electrokinetic effects and preventing exosomes from moving through the microchannel.

Numerical simulations confirmed the generation of different magnitudes of the electric field gradient and DEP force in each section. The separated exosomes were subsequently released and recovered using electroosmotic flow via the side channels.

While further optimization and functionalization of the device are necessary, this technology holds potential for the development of high-throughput, fast, and robust microfluidic systems that can concentrate and separate exosomes from complex biological mixtures, leading to advancements in exosome-based therapeutics and diagnostics.

III. Development of a Hydrogel System for the Controlled Delivery of Exosomes

A. Introduction

Local and controlled delivery of exosomes employing hydrogels can improve the efficacy of exosome-based therapeutics [18]. Alginate hydrogels have gained attention as drug delivery systems due to their biocompatibility and cargo loading capacity [19], [20]. However, alginate hydrogels are highly stable in solution and not easily injectable.

The degradation rate of alginate hydrogels can be controlled by oxidation, allowing increased degradability [21]. Biodegradable hydrogels eliminate the need for removal after exosome release, making them advantageous for bioactive delivery. Alginate can also be modified by methacrylation, enabling gelation upon exposure to UV light [22], [23].

Photocrosslinked alginate hydrogels have shown tailorable physicochemical properties and therefore, versatility in their use. The properties of oxidized and methacrylated alginate hydrogels can be tuned by varying the degree of alginate oxidation and methacrylation, macromer concentration, and crosslinking density [24]. Therefore, these hydrogels promise to be a suitable vehicle for the controlled delivery of exosomes.

Because of the ongoing publication process of this work, the experimental, results and discussion, and conclusions sections, as well as the data associated to this study have not been included.

However, the following sections provide an overview of the objectives and scope of our work, as well as perspectives into the use hydrogels to design delivery systems for the controlled delivery of EVs.

B. Objectives and scope

For this work, our aim was to produce alginate hydrogels with different alginate oxidation degrees to control the degradation rate. The swelling kinetics, degradation rate and mechanical stability of photocrosslinked alginate hydrogels were investigated. Cancer cell-derived exosomes were encapsulated in alginate hydrogels designed for rapid or slow degradation, and the release rate was evaluated (Fig. 6). The biocompatibility of the hydrogels and their ability to deliver functional exosomes *in vitro* were also assessed.

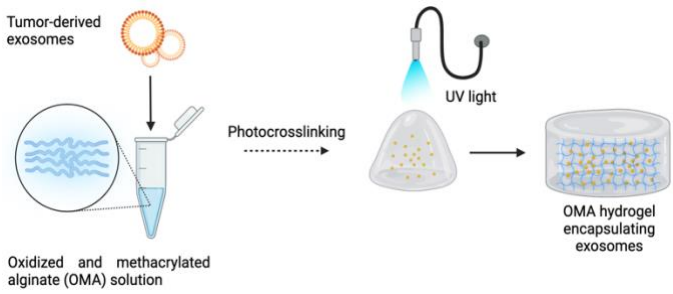

Figure 6. A general schematic of the development of oxidized and methacrylated alginate hydrogels for the controlled delivery of exosomes.

C. Future perspectives

Hydrogel systems can be tuned to modulate the release of the exosomes based on their physicochemical properties or environmental cues [18,19]. By combining the unique properties of exosomes with hydrogels, it may be possible to develop more effective and safe therapeutics for cancer treatment.

Currently, the toxicity and disease control rate of exosome-based therapeutics remains largely unknown. Previous studies on the use of EVs as therapeutics have explored a wide range of delivery mechanisms, such as oral administration, inhalation, topical application, and intraperitoneal injection [25], [26]. However, these show high accumulation of EVs in a single tissue, rapid uptake by macrophages and off-target effects.

This study highlights the possibility of developing hydrogel systems for the controlled release of these EVs, improving their efficacy and safety. An optimal delivery system would release EVs at a predetermined rate for a specified period. In this context, a complex hydrogel system may show more controllability [27]. However, reducing the complexity of the biomaterial, while controlling the release rate remains a relevant aim for specific applications.

Because of the controllable release behavior of hydrogels, these can be proposed as delivery vehicles for exosomes in various medical fields. For instance, there is a current trend to develop injectable hydrogels to suppress tumor growth by the local delivery of therapeutics that may cause serious side effects if administer systemically [28], [29].

Chao *et al*., developed an alginate-based delivery system for localized chemotherapy with immune adjuvants that can be combined with conventional intravenous injection of immune check point inhibitors [30]. These strategies have shown great potential for clinical translation and support the rationality of including exosomes into these systems for drug delivery and antitumor immunity.

Hydrogel-based local delivery of immune checkpoint blockade therapy, immune cell therapy, tumor vaccines, and oncolytic viruses are emerging as promising modalities of anticancer therapy that also facilitate combination therapies [31]–[33]. Progress on the development of these systems may shed light on their specific applications and would certainly be worth of further investigation.

IV. Development of a 3D cell culture model to study exosome biology

A. Introduction

PD-L1 (programmed death-ligand 1) is a protein found on the surface of cancer cells, which binds to the immune cell receptor PD-1, promoting immune evasion and tumor progression [34]. Proinflammatory cytokines, such as interferon-gamma (IFN-γ) can stimulate the expression of PD-L1 in various cell types [35]. However, the mechanisms regulating PD-L1 expression remain to be fully elucidated.

Immune checkpoint inhibitors (ICIs) that block the interaction between PD-L1 and PD-1 have significantly improved the clinical outcomes of patients with advanced cancer [36], [37]. Furthermore, evaluating PD-L1 expression in tumor cells is important to identify patients who may benefit from ICIs, and to predict their therapeutic efficacy [38].

Recent studies have suggested that extracellular forms of PD-L1, including PD-L1 associated with EVs such as exosomes, play a key role in tumor progression and therapeutic resistance [39]. Therefore, exosome blockade has been suggested as a therapeutic strategy to improve the efficacy of immunotherapy.

GW4869 is a pharmacological inhibitor that blocks exosome generation by targeting the ceramide biosynthesis pathway [13]. Recent studies have shown that inhibiting exosome release can downregulate both membrane PD-L1 and the level of exosomal PD-L1 [40]. However, contrasting findings have also been reported, suggesting that GW4869 can increase membrane PD-L1 expression while decreasing exosomal PD-L1 release [41].

Here, we employed A549 lung adenocarcinoma cells to investigate PD-L1 expression and extracellular release during proinflammatory stimulation and exosome blockade and to compare the performance of monolayer cell culture with 3D cell culture, which better replicates the complexity of the tumor microenvironment.

This study highlights the importance of understanding PD-L1 subcellular localization and exosome biology in different cell culture models. It also provides a foundational model for future research aimed at improving our understanding of these processes, which could potentially contribute to the development of more effective therapeutic strategies for cancer care.

B. Experimental section

Cell culture. The A549 cell line was cultured in DMEM/F12 medium with 10% FBS and 1% penicillin/streptomycin. IFN-γ (100 ng/mL) was added to the media for 72 hours to induce PD-L1 expression. GW4869 (40 μM) was added to media for 72 hours to inhibit exosome release. GW4869 was dissolved in DMSO and diluted in PBS with a final DMSO concentration of 0.4% (v/v). DMSO was used as vehicle control.

Generation of tumor spheroids. A549 spheroids were generated in ultra-low attachment (ULA) round bottom 96-well plates by seeding single cell suspensions. Viability of A549 spheroids was evaluated using a Live/Dead assay, and images were captured using a fluorescence microscope.

Flow cytometry**.** To detect PD-L1 cell surface protein expression, A549 cells in monolayer culture were detached using trypsin-EDTA solution. For A549 spheroids, harvested spheroids were dissociated into single cells using trypsin-EDTA solution. The cells were then stained with an APC-conjugated PD-L1 antibody and discriminated for live and

dead cells using propidium iodine. Flow cytometry was performed using a BD FACSCanto II instrument, and data analysis was conducted using FlowJo software. Results were expressed as the specific mean fluorescence intensity (MFI) of the experimental conditions relative to the specific fluorescence of controls based on the nonspecific fluorescence of unstained cells.

Exosome isolation and characterization. EVs from A549 cell culture supernatants were recovered using the ExoQuick-TC exosome precipitation solution, as previously described [17]. The protein concentration of the EV samples was determined using a NanoDrop 2000 spectrophotometer (Thermo Scientific, Waltham, MA, USA). Dynamic light scattering (DLS) was performed using a ZetaSizer Nano ZS (Malvern Instruments, UK) to measure the diameter of EVs. To quantify the level of CD63 in the EVs, the ExoELISA-Ultra CD63 kit (System Biosciences, USA) was used according to the manufacturer's protocol.

PD-L1 ELISA. To quantify the total extracellular PD-L1 concentration in cell culture medium, the human PD-L1 ELISA Kit (ab277712, Abcam, USA) was used according to the manufacturer's protocol.

Cell proliferation. The proliferation of A549 cells was measured by the CellTiter 96 AQ One Solution cell proliferation assay (Promega, USA), as indicated by the manufacturer.

Statistics. Data indicates means and standard error. Statistical significance was defined as $*p<0.05$; $**p<0.005$; $***p<0.0005$; $****p<0.0001$. Statistical analysis between two groups was compared using an unpaired two-tailed Student's t test. Statistics analysis among multiple groups was compared using a one-way analysis of variance (ANOVA) with the Tukey significant difference post hoc test or a two-way ANOVA with Sidak's multiple comparison test, as indicated. GraphPad Prism 6.0 (GraphPad Software Inc., USA) was used for statistical analyses and graph generation.

C. Results and discussion

IFN-γ significantly increased PD-L1 expression as indicated by the mean fluorescence intensity (MFI) corresponding to PD-L1 in cells treated with IFN-γ and GW4869 (12.18 ± 4.45), and in cells treated with IFN-γ and DMSO (12.69 ± 1.36) relative to control cells (1.00 ± 0.13), (Fig 7A and B). Conversely, the MFI corresponding to PD-L1 did not show a significant increase after incubation with GW4869 (1.36 ± 0.70) or DMSO, (1.11 ± 0.10) relative to control cells.

Accordingly, our findings show that the constitutive PD-L1 expression at the cell surface of A549 cells is inherently low, but it was effectively increased after IFN-γ treatment. Our data also suggest that GW4869 did not influence PD-L1 expression during IFN-γ stimulation.

As seen in Fig. 7C, the extracellular concentration of PD-L1 in the medium of control cells was 29.36 ± 5.34 pg/mL, and this did not significantly change with GW4869 or DMSO treatment (18.08 ± 1.28 pg/mL and 18.42 ± 1.39 pg/mL, respectively).

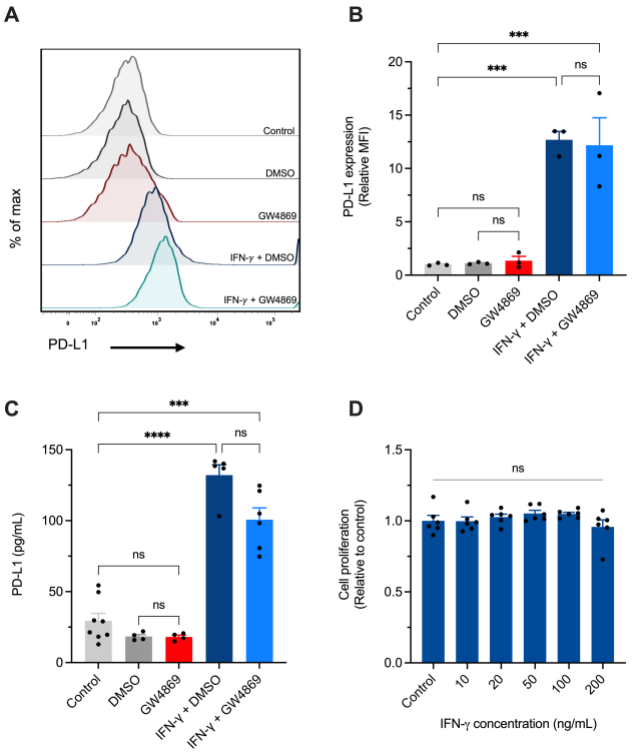

Fig. 7. IFN-γ upregulates PD-L1 expression and increases the level of extracellular PD-L1 in A549 lung adenocarcinoma cells. (A) Representative histograms of PD-L1 expression measured using flow cytometry and (B) relative mean fluorescence intensity (MFI) of PD-L1 in tumor cells. (C) Extracellular PD-L1 concentration in A549 cell culture supernatant assayed by ELISA (D) Cell proliferation of A549 cells treated with increasing concentrations of IFN-γ.

However, treatment with IFN-γ significantly increased the release of extracellular PD-L1 (132.10 ± 7.31 pg/mL), and this effect was still observed with GW4869 treatment (100.73 ± 8.34 pg/mL). Additionally, different concentrations of IFN-γ (10-200 ng/mL) did not significantly affect cell proliferation compared to the control group (Fig. 7D).

DLS analysis revealed that EVs from untreated cells had a particle diameter of 129.16 ± 28.81 nm (Fig. 8A). Notably, GW4869 significantly reduced protein concentration in EVs (3.46 ± 0.13 µg/µL), when compared to both the control (4.71 ± 0.22 µg/µL) and DMSO groups (4.26 ± 0.70 µg/µL) (Fig. 8B). This effect persisted even when IFN-γ was added concurrently with GW4869, reducing the protein concentration in EVs to 4.01 ± 0.22 µg/µL, compared to the IFN-γ and DMSO groups (5.15 ± 0.22 µg/µL).

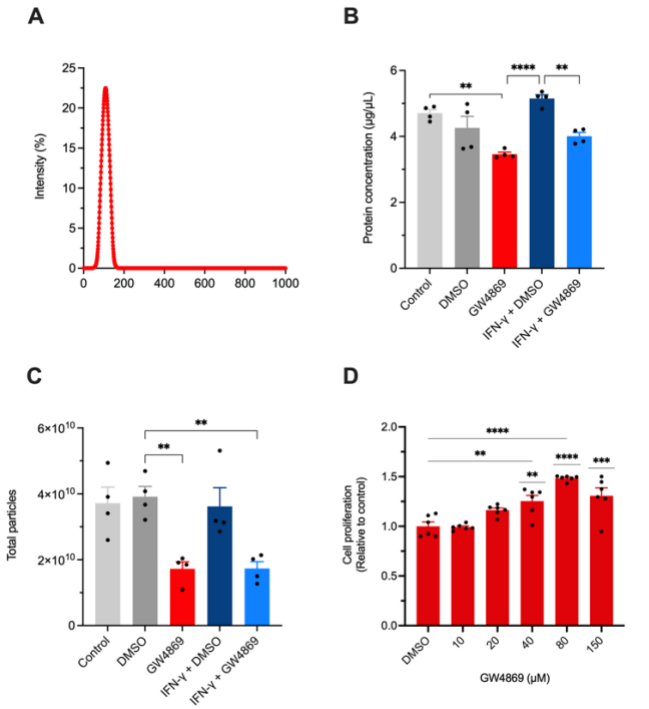

Fig. 8. The effect of GW4869 on extracellular vesicle protein content, CD63 level, and cell proliferation. (A) Representative histogram depicting the particle hydrodynamic diameter. (B) The total protein content and (C) particle number relative to the amount of CD63 in EVs. (D) Cell proliferation of A549 cells after incubation with increasing concentrations of GW4869.

These findings suggest that GW4869 can reduce the protein concentration of EVs during immunostimulation. However, it should be noted that the protein content of EV samples is not a specific marker of exosome secretion, and these changes may be attributed to a variety of cellular processes.

The level of CD63, a classical exosome marker, in EVs was evaluated by ELISA calibrated to particle concentration via NTA. The resulting absorbance corresponding to CD63 was found to correlate to $3.72 \times 10^{10} \pm 9.76 \times 10^{9}$ particles in control cells (Fig 8C). After incubation with GW4869, there was a significant reduction in the total number of particles to $1.72 \times 10^{10} \pm 4.31 \times 10^{9}$, compared to both control cells and those treated with DMSO. These findings suggest that GW4869 effectively inhibits exosome release from A549 cells, and this effect is sustained in the presence of IFN-γ.

As shown in Fig. 8D, a significant increase in cell proliferation was noted after incubation with GW4869 at concentrations of 40 µM, 80 µM and 150 µM, when compared to control. These findings underscore the potential of GW4860 in not only modulating EV release but also in promoting cell proliferation.

In this study, we used spheroids as a proof-of-concept model to study the expression and subcellular localization of PD-L1 in 3D cell culture. Spheroids were produced by seeding A549 cells in ultra-low attachment plates (Fig. 9).

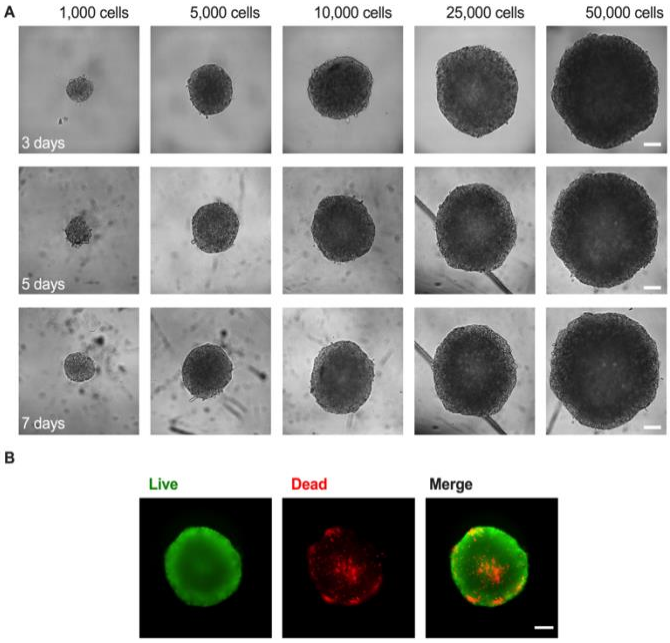

Fig. 9. Characterization of A549 spheroids. (A) Representative phase-contrast images of A549 spheroids at different seeding densities and time points and (B) Typical fluorescence images of A549 spheroids after live/dead staining. Scale bar: 200 µm

The formation of cell aggregates was observed after 12 h, regardless of initial seeding density. After 48 h, the compactness of these aggregates considerably increased. By day 3, spheroids produced from over 10,000 initial cells had formed. The initial cell density was found to correlate with the spheroid size, as shown in Fig 9A.

These spheroids presented a uniform size and sphericity and were considered suitable for further experimentation. Moreover, these spheroids showed a proliferative zone encompassing a necrotic core (Fig. 9B). After 7 days, the spheroids maintained stable morphology and size.

As shown in Fig 10A and B, the intrinsic PD-L1 expression at the cell membrane of spheroids was low, similar to A549 cells grown in a monolayer. Importantly, no significant differences were observed in the MFI between the control group of monolayer culture and spheroids.

PD-L1 expression on the cell surface was not significantly affected by GW4869 or DMSO, indicating similarity between culture models. Additionally, GW4869 did not alter the extracellular PD-L1 concentration, even during IFN-γ stimulation (Fig. 10C).

Nonetheless, the fold-change increase in extracellular PD-L1 induced by IFN-γ was higher in spheroids compared to monolayer culture (Fig. 10D). These findings suggest that tumor spheroids could be a better model for studying the secretome of cancer cells.

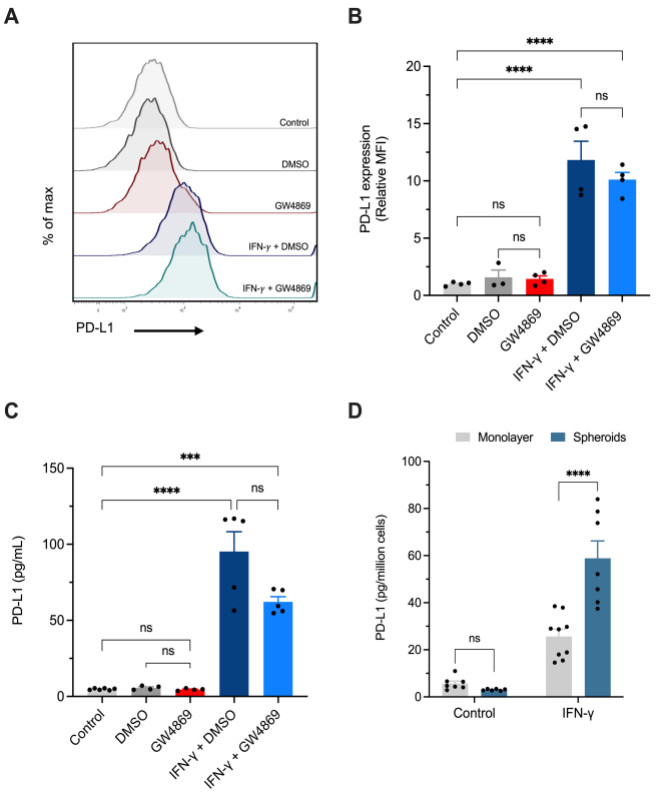

Fig. 10. The effect of IFN-γ and GW4869 on membrane PD-L1 expression and extracellular release in tumor spheroids. (A) Representative histograms of PD-L1 expression measured using flow cytometry and (B) relative mean fluorescence intensity (MFI) of PD-L1 in tumor cells. (C) Extracellular PD-L1 concentration in A549 cell culture supernatant assayed by ELISA. (D) PD-L1 content per million cells in the culture medium of A549 monolayer culture and spheroids after incubation with IFN-γ.

In summary, we found that blocking exosome release with GW4869 did not significantly affect membrane-bound PD-L1 expression or extracellular release of PD-L1, despite upregulation by IFN-γ. These findings highlight the role of proinflammatory cytokines in tumor immune evasion and suggest that blocking exosome release may not influence the therapeutic efficacy of ICIs or PD-L1 detection.

It should be noted that alternative pathways and other forms of extracellular PD-L1 may still be involved. Despite the insights gained, further research is needed to explore specific effects on exosomal PD-L1, assess PD-L1 expression in other compartments, and consider the complexity of the tumor microenvironment to develop a more advance 3D cell culture model.

D. Conclusion

Our findings shed light on the interplay between immune response, exosome biogenesis, and culture models. Further research in this area can improve our understanding of tumor immune evasion and inform the development of more effective therapies.

V. General Conclusions and Recommendations

Exosome research holds great potential for cancer diagnostics and therapeutics, but there are significant challenges in translating this technology into clinical applications. Ongoing clinical trials and the development of exosome-based products are underway, but there is still much work needed to ensure their safety and effectiveness for clinical use.

Proper isolation of exosomes is crucial for accurate study and application, and microdevices show promise in standardizing and simplifying this process. These devices can enable faster and more affordable diagnostic tests, making them suitable for point-of-care applications.

Hydrogel systems show potential in enhancing exosome pharmacokinetics and targeting, but their biocompatibility and efficacy also need thorough evaluation. Likewise, 3D cell culture models are proposed as the next generation drug screening platforms, but the establishment of advanced models that convey clinically relevant data remains challenging.

Collaboration between researchers, academia, industry, and regulatory agencies is essential for advancing exosome research and ensuring standardization, reproducibility, and compliance with regulatory requirements. Continued investment and a multidisciplinary approach are needed to fully realize the potential of exosomes in cancer prevention, diagnosis, and treatment.

Acknowledgment

We thank the School of Engineering and Science at Tecnológico de Monterrey for its support through the Molecular and Systems Bioengineering and the Nano-sensors and Devices Research Groups, as well as the FEMSA-Biotechnology Center.

We also thank the School of Medicine and Health Sciences at Tecnológico de Monterrey for its support through the Cardiology and Vascular Health Research Group. The authors would like to thank Eben Alsberg and the University of Illinois at Chicago for their valuable contributions to this research and their ongoing collaboration.

Sergio Ayala-Mar thanks the National Council on Science and Technology of Mexico (CONACyT) for scholarship number 850524. Some figures were created with BioRender.com.

References

[1] L. Cheng and A. F. Hill, "Therapeutically harnessing extracellular vesicles," *Nat. Rev. Drug Discov.*, vol. 21, no. 5, pp. 379–399, 2022.

[2] D. Zheng *et al.*, "Advances in extracellular vesicle functionalization strategies for tissue regeneration," *Bioact. Mater.*, 2022.

[3] M. Ramirez-Garrastacho *et al.*, "Extracellular vesicles as a source of prostate cancer biomarkers in liquid biopsies: a decade of research," *Br. J. Cancer*, vol. 126, no. 3, pp. 331–350, 2022.

[4] S. N. Bhatia, X. Chen, M. A. Dobrovolskaia, and T. Lammers, "Cancer nanomedicine," *Nat. Rev. Cancer*, vol. 22, no. 10, pp. 550–556, 2022.

[5] I. Kimiz-Gebologlu and S. S. Oncel, "Exosomes: Large-scale production, isolation, drug loading efficiency, and biodistribution and uptake," *J. Control. Release*, vol. 347, pp. 533–543, 2022.

[6] J. Rezaie, M. Feghhi, and T. Etemadi, "A review on exosomes

application in clinical trials: Perspective, questions, and challenges," *Cell Commun. Signal.*, vol. 20, no. 1, pp. 1–13, 2022.
[7] F. Malekian, A. Shamsian, S. P. Kodam, and M. Ullah, "Exosome engineering for efficient and targeted drug delivery: Current status and future perspective," *J. Physiol.*, 2022.
[8] B. Lin *et al.*, "Microfluidic-Based Exosome Analysis for Liquid Biopsy.," *Small methods*, vol. 5, no. 3, p. e2001131, Mar. 2021, doi: 10.1002/smtd.202001131.
[9] Y. W. Yi *et al.*, "Advances in Analysis of Biodistribution of Exosomes by Molecular Imaging," *Int. J. Mol. Sci.*, vol. 21, no. 2, p. 665, Jan. 2020, doi: 10.3390/ijms21020665.
[10] Y. S. Zhang and A. Khademhosseini, "Advances in engineering hydrogels," *Science (80-.).*, vol. 356, no. 6337, p. eaaf3627, May 2017, doi: 10.1126/science.aaf3627.
[11] S. Nath and G. R. Devi, "Three-dimensional culture systems in cancer research: Focus on tumor spheroid model," *Pharmacol. Ther.*, vol. 163, pp. 94–108, 2016, doi: https://doi.org/10.1016/j.pharmthera.2016.03.013.
[12] Q. Tang *et al.*, "Tumor-derived exosomes in the cancer immune microenvironment and cancer immunotherapy," *Cancer Lett.*, vol. 548, p. 215823, 2022, doi: https://doi.org/10.1016/j.canlet.2022.215823.
[13] H. Zhang, J. Lu, J. Liu, G. Zhang, and A. Lu, "Advances in the discovery of exosome inhibitors in cancer," *J. Enzyme Inhib. Med. Chem.*, vol. 35, no. 1, pp. 1322–1330, Jan. 2020, doi: 10.1080/14756366.2020.1754814.
[14] A. Liga, A. D. B. Vliegenthart, W. Oosthuyzen, J. W. Dear, and M. Kersaudy-Kerhoas, "Exosome isolation: A microfluidic road-map," *Lab Chip*, vol. 15, no. 11, pp. 2388–2394, 2015, doi: 10.1039/c5lc00240k.
[15] R. C. Gallo-Villanueva, V. H. Pérez-González, R. V. Davalos, and B. H. Lapizco-Encinas, "Separation of mixtures of particles in a multipart microdevice employing insulator-based dielectrophoresis," *Electrophoresis*, vol. 32, pp. 2456–2465, 2011, doi: 10.1002/elps.201100174.
[16] N. Abd Rahman, F. Ibrahim, and B. Yafouz, "Dielectrophoresis for Biomedical Sciences Applications: A Review.," *Sensors (Basel).*, vol. 17, no. 3, Mar. 2017, doi: 10.3390/s17030449.
[17] S. Ayala-Mar, V. H. Perez-Gonzalez, M. A. Mata-Gómez, R. C. Gallo-Villanueva, and J. González-Valdez, "Electrokinetically Driven Exosome Separation and Concentration Using Dielectrophoretic-Enhanced PDMS-Based Microfluidics," *Anal. Chem.*, 2019, doi: 10.1021/acs.analchem.9b03448.
[18] W. Jing *et al.*, "Metabolic Modulation of Intracellular Ammonia via Intravesical Instillation of Nanoporter-Encased Hydrogel Eradicates Bladder Carcinoma.," *Adv. Sci. (Weinheim, Baden-Wurttemberg, Ger.)*, p. e2206893, Feb. 2023, doi: 10.1002/advs.202206893.
[19] J. Li *et al.*, "Long-term functional regeneration of radiation-damaged salivary glands through delivery of a neurogenic hydrogel," *Sci. Adv.*, vol. 8, no. 51, p. eadc8753, Feb. 2023, doi: 10.1126/sciadv.adc8753.
[20] Y. Zhang *et al.*, "Hydrogel-load exosomes derived from dendritic cells improve cardiac function via Treg cells and the polarization of macrophages following myocardial infarction.," *J. Nanobiotechnology*, vol. 19, no. 1, p. 271, Sep. 2021, doi: 10.1186/s12951-021-01016-x.
[21] K. H. Bouhadir, K. Y. Lee, E. Alsberg, K. L. Damm, K. W. Anderson, and D. J. Mooney, "Degradation of partially oxidized alginate and its potential application for tissue engineering," *Biotechnol. Prog.*, vol. 17, no. 5, pp. 945–950, 2001.
[22] O. Jeon, T.-H. Kim, and E. Alsberg, "Reversible dynamic mechanics of hydrogels for regulation of cellular behavior," *Acta Biomater.*, vol. 136, pp. 88–98, 2021, doi: https://doi.org/10.1016/j.actbio.2021.09.032.
[23] O. Jeon, D. S. Alt, S. M. Ahmed, and E. Alsberg, "The effect of oxidation on the degradation of photocrosslinkable alginate hydrogels," *Biomaterials*, vol. 33, no. 13, pp. 3503–3514, 2012, doi: https://doi.org/10.1016/j.biomaterials.2012.01.041.
[24] O. Jeon, J. E. Samorezov, and E. Alsberg, "Single and dual crosslinked oxidized methacrylated alginate/PEG hydrogels for bioadhesive applications," *Acta Biomater.*, vol. 10, no. 1, pp. 47–55, 2014, doi: https://doi.org/10.1016/j.actbio.2013.09.004.
[25] K. D. Popowski *et al.*, "Inhalable exosomes outperform liposomes as mRNA and protein drug carriers to the lung.," *Extracell. vesicle*, vol. 1, p. 100002, Dec. 2022, doi: 10.1016/j.vesic.2022.100002.
[26] H. Pak *et al.*, "Safety and efficacy of injection of human placenta mesenchymal stem cells derived exosomes for treatment of complex perianal fistula in non-Crohn's cases: Clinical trial phase I.," *J. Gastroenterol. Hepatol.*, Jan. 2023, doi: 10.1111/jgh.16110.
[27] S. S. Yerneni *et al.*, "Controlled release of exosomes using atom transfer radical polymerization-based hydrogels," *Biomacromolecules*, vol. 23, no. 4, pp. 1713–1722, 2022.
[28] H. Zhang, J. Zhang, Y. Liu, Y. Jiang, and Z. Li, "Molecular Targeted Agent and Immune Checkpoint Inhibitor Co-Loaded Thermosensitive Hydrogel for Synergistic Therapy of Rectal Cancer ," *Frontiers in Pharmacology* , vol. 12. 2021. [Online]. Available: https://www.frontiersin.org/articles/10.3389/fphar.2021.671611
[29] W. Li *et al.*, "An orally available PD-1/PD-L1 blocking peptide OPBP-1-loaded trimethyl chitosan hydrogel for cancer immunotherapy," *J. Control. Release*, vol. 334, pp. 376–388, 2021, doi: https://doi.org/10.1016/j.jconrel.2021.04.036.
[30] Y. Chao *et al.*, "Localized cocktail chemoimmunotherapy after in situ gelation to trigger robust systemic antitumor immune responses.," *Sci. Adv.*, vol. 6, no. 10, p. eaaz4204, Mar. 2020, doi: 10.1126/sciadv.aaz4204.
[31] H. Zheng *et al.*, "Progress in the application of hydrogels in immunotherapy of gastrointestinal tumors," *Drug Deliv.*, vol. 30, no. 1, p. 2161670, Dec. 2023, doi: 10.1080/10717544.2022.2161670.
[32] F. Yang *et al.*, "Cyclophosphamide loaded thermo-responsive hydrogel system synergize with a hydrogel cancer vaccine to amplify cancer immunotherapy in a prime-boost manner.," *Bioact. Mater.*, vol. 6, no. 10, pp. 3036–3048, Oct. 2021, doi: 10.1016/j.bioactmat.2021.03.003.
[33] S. Deng *et al.*, "Development of a New Hyaluronic Acid Based Redox-Responsive Nanohydrogel for the Encapsulation of Oncolytic Viruses for Cancer Immunotherapy.," *Nanomater. (Basel, Switzerland)*, vol. 11, no. 1, Jan. 2021, doi: 10.3390/nano11010144.
[34] S. Bagchi, R. Yuan, and E. G. Engleman, "Immune Checkpoint Inhibitors for the Treatment of Cancer: Clinical Impact and Mechanisms of Response and Resistance.," *Annu. Rev. Pathol.*, vol. 16, pp. 223–249, Jan. 2021, doi: 10.1146/annurev-pathol-042020-042741.
[35] L. Cucolo *et al.*, "The interferon-stimulated gene RIPK1 regulates cancer cell intrinsic and extrinsic resistance to immune checkpoint blockade.," *Immunity*, vol. 55, no. 4, pp. 671-685.e10, Apr. 2022, doi: 10.1016/j.immuni.2022.03.007.
[36] R. I. Haddad *et al.*, "Influence of tumor mutational burden, inflammatory gene expression profile, and PD-L1 expression on response to pembrolizumab in head and neck squamous cell carcinoma.," *J. Immunother. cancer*, vol. 10, no. 2, Feb. 2022, doi: 10.1136/jitc-2021-003026.
[37] V. Kloten, R. Lampignano, T. Krahn, and T. Schlange, "Circulating Tumor Cell PD-L1 Expression as Biomarker for Therapeutic Efficacy of Immune Checkpoint Inhibition in NSCLC," *Cells*, vol. 8, no. 8. 2019. doi: 10.3390/cells8080809.
[38] A. J. Schoenfeld *et al.*, "Clinical and molecular correlates of PD-L1 expression in patients with lung adenocarcinomas☆," *Ann. Oncol.*, vol. 31, no. 5, pp. 599–608, 2020, doi: https://doi.org/10.1016/j.annonc.2020.01.065.
[39] M. Poggio *et al.*, "Suppression of Exosomal PD-L1 Induces Systemic Anti-tumor Immunity and Memory," *Cell*, vol. 177, no. 2, pp. 414-427.e13, 2019, doi: 10.1016/j.cell.2019.02.016.
[40] J. Monypenny *et al.*, "ALIX Regulates Tumor-Mediated Immunosuppression by Controlling EGFR Activity and PD-L1 Presentation," *Cell Rep.*, 2018, doi: 10.1016/j.celrep.2018.06.066.
[41] D.-D. Shen *et al.*, "LSD1 deletion decreases exosomal PD-L1 and restores T-cell response in gastric cancer," *Mol. Cancer*, vol. 21, no. 1, p. 75, 2022, doi: 10.1186/s12943-022-01557-1.